

Unloading of cryoprotectants from cryoprotectant-loaded cells on a microfluidic platform

Yufeng Kang^{1,2} · Lili Zou^{1,2} · Bensheng Qiu^{1,2} · Xin Liang^{1,2} · Sijie Sun³ · Dayong Gao⁴ · Weiping Ding^{1,2}

Published online: 28 February 2017
© Springer Science+Business Media New York 2017

Abstract In this paper, a multistep dilution-filtration microdevice (MDFD) is developed for unloading cryoprotectants from cryoprotectant-loaded cells. The MDFD contained a diluent producing region, a dilution-filtration execution region, and a filtrate collection region. It was made of two patterned PMMA stamps with four pieces of sandwiched PVDF membranes. Firstly, the performances of the mixers that were used in the diluent producing region and the dilution-filtration execution region were assessed using fluorescence experiments. Then, the effect of the MDFD structure on the loss of cells was investigated by applying the MDFD to unload glycerin from glycerin-loaded porcine red blood cells. Finally, the effects of the cell density, glycerin concentration, and membrane pore size on the clearance efficiency of glycerin (C_G), the survival rate of cells (S_C) and the recovery rate of cells (R_C) have been studied. Under the designed conditions, C_G achieved ~80% and S_C reached ~90%. However, R_C was only ~40%, mainly resulting from the cells detained on the membrane surface and squeezed through the membrane pores into the filtrate. Increasing the membrane pore size caused high C_G

and S_C , but low R_C . For a low glycerin concentration, C_G , S_C , and R_C were all high. For a high cell density, C_G was high, but both S_C and R_C were low. This work is of significance to develop a microfluidic chip for unloading cryoprotectants from a small amount of cryopreserved cell samples.

Keywords Microfluidic · Cryoprotectant · Deglycerolization · Dilution · Filtration

1 Introduction

Cryopreservation is a routine way to increase the shelf life of cells (Meryman 2007; Zhang et al. 2010). Today, the cryopreserved cells have been widely used in cell therapy (Fitzpatrick et al. 2015; Hubel 2011; Yong et al. 2015), reproductive medicine (Ferrari et al. 2016; Jadoon and Adeel 2015; Wang et al. 2016) and so on. In cryopreservation, a specific cryoprotectant (CPA) is loaded into cells to prevent cells from cryoinjury, but it must be removed before clinical use because of negative effects, such as diarrhea, acute hypotension, and ischemic cerebrovascular disease (Almansoori et al. 2012; Hoyt et al. 2000; Syme et al. 2004). Many approaches have been proposed to unload CPAs from cryopreserved cells. However, existing approaches, such as centrifugation-based (Lusianti et al. 2013), dialysis-based (Ding et al. 2007) and filtration-based methods (Zhou et al. 2011) are designed mainly to process large volume cell samples (30 ~ 500 mL) (Mata et al. 2009) and not suitable for small volume cell samples. Microfluidic, as a burgeoning and promising technology has been widely used to manipulate small volume biological samples (Burg et al. 2007; Dou et al. 2015; Ragsdale et al. 2016), and also makes it possible to load CPAs into and unload CPAs from a small amount of cells (Heo et al. 2011; Mata et al. 2008; Song et al. 2009).

Electronic supplementary material The online version of this article (doi:10.1007/s10544-017-0155-6) contains supplementary material, which is available to authorized users.

✉ Weiping Ding
wpdings@ustc.edu.cn

- ¹ Center for Biomedical Engineering, University of Science and Technology of China, Hefei, Anhui 230027, China
- ² Department of Electronic Science and Technology, University of Science and Technology of China, Hefei, Anhui 230027, China
- ³ Department of Laboratory Medicine, University of Washington, Seattle, WA 98195, USA
- ⁴ Department of Mechanical Engineering, University of Washington, Seattle, WA 98195, USA

Nowadays, studies mainly focus on the loading of CPAs into cells on chips (Heo et al. 2011; Park et al. 2011; Pyne et al. 2014; Scherr et al. 2014; Song et al. 2009), but few are related to the unloading of CPAs from cells. Hubel's team (Fleming Glass et al. 2008; Hanna et al. 2012; Longmire 2006; Mata et al. 2009; Mata et al. 2008) and Demirci's team (Song et al. 2009) developed diffusion-based microfluidic devices to unload CPAs. Their designs are very promising, but further improvement is still needed because of low DMSO extraction efficiency (generally less than 60%). In addition, their microdevices may be not suitable for removing glycerin from glycerin-loaded cells because of the differences in the molecular diffusivity and the cell membrane permeability (Fleming Glass et al. 2008). Higgins's team proposed a dialysis-based microdevice to remove glycerin from glycerolized blood (Lusianti and Higgins 2014). For a single device, the clearance of glycerin was approximately 50%. To further increase the clearance of glycerin, they also designed a multistep microdialysis process theoretically. In our previous work (Zhou et al. 2011), a dilution-filtration system was proposed to remove glycerin from cryopreserved blood. In the system, the red blood cell suspension is diluted and filtrated continuously and simultaneously, and thus the glycerin in cells is removed gradually. Later, we theoretically optimized the system further to reduce the osmotic damage to cells and to shorten the washing time of glycerin (Gong et al. 2013; Qiao et al. 2014). This system is suitable for large volume blood or cell suspension, but not for a small amount of cryopreserved cells.

Therefore, the aim of this study is to develop a multistep dilution-filtration microdevice (MDFD) to unload CPAs from a small amount of CPA-loaded cells. The MDFD is based on the dilution-filtration concept, but it is not a miniaturized device of the previously developed macro-system. In the MDFD, a unique design is included to produce dilution solutions with various NaCl concentrations and to dilute the CPA-loaded cell suspension at various flow rates, making the CPA unloading process totally automatic. We sketch the design of the MDFD and assess the performance of the MDFD by applying the MDFD to remove glycerin from the glycerin-loaded porcine red blood cells. This work can provide some insights into the integrated design for unloading CPAs from CPA-loaded cells on biochips.

2 Materials and methods

2.1 MDFD design

In the design of the MDFD (Fig. 1), the core idea was: the cell suspension with CPAs was diluted by NaCl solutions and then the diluted extracellular solution with CPAs was removed by filtration. To avoid the osmotic damage to cells induced by the excessive change in the volume of cells, the hypertonic

diluents were adopted in the 1st and 2nd dilution processes (the hypotonic diluent was used in the 3rd and 4th dilution processes to recover the cell volume to the isotonic cell volume).

The MDFD contained a diluent producing region, a dilution-filtration execution region, and a filtrate collection region. It consisted of two patterned stamps with four pieces of sandwiched membranes (Fig. 1a, b): the diluent producing region and the filtrate collection region were located on the upper stamp; the dilution-filtration execution region was designed on both upper and lower stamps in the corresponding position (the passage of the cell suspension was located on the lower stamp); and the membranes were sandwiched in the dilution-filtration execution region.

In operation, the cell suspension, hypertonic solution (i.e. concentrated NaCl solution) and deionized water were introduced to **IN1**, **IN2** and **IN3**, respectively, the washed cell suspension was collected from **OUT1**, and the filtrates (the extracellular solutions through the filtration membrane) was collected from **OUT2** (Fig. 1b and c). Four diluents with desired NaCl concentrations were generated in the diluent producing region and then introduced to the dilution points at desired flow rates using a ladder network to mix deionized water (DI) and concentrated NaCl solution (Kim et al. 2008). When the cell suspension flowed through the dilution-filtration execution region, it was diluted by diluents at the dilution points and concentrated during the membrane filtration process. Thus, the CPA in the cell suspension was gradually removed by collecting and discarding the filtrates.

2.2 MDFD fabrication

The two patterned stamps were fabricated with Poly-Methyl-Methacrylate (PMMA) at Suzhou Wenhao Chip Technology Co. Ltd., Suzhou, China. In this work, the hypertonic solution was 20% (w/v) NaCl solution and the flow rates through **IN1**, **IN2**, and **IN3** were fixed at 0.200 mL/min, 0.188 mL/min and 1.212 mL/min, respectively. The NaCl concentrations in four diluents were designed to be 12%, 2.4%, 0.85% and 0.6% (w/v), respectively. The ratios of the dilution solution flow rate to the cell suspension flow rate at four stages were designed to be 1.0, 1.5, 2.0, and 2.5, respectively (the filtrate flow rate was designed to be the same as the diluent flow rate at all stages). The schematic of the flow resistance networks of the MDFD is used to calculate the design parameters (Fig. S1). The designed lengths and widths of fluid pathways are listed in Table S1 (the heights were 500 μm ; the flow network design was based on the Kirchhoff's current and voltage laws (Kim et al. 2008); see [Supplementary Information](#)). The size of the groove used for filtration (Fig. 1b; dashed red ellipse) was 15 mm \times 5 mm. The size of 4 micro-posts for the membrane support was 1 mm \times 1 mm and the center distance between two micro-posts was 2 mm. The diameter of the dilution

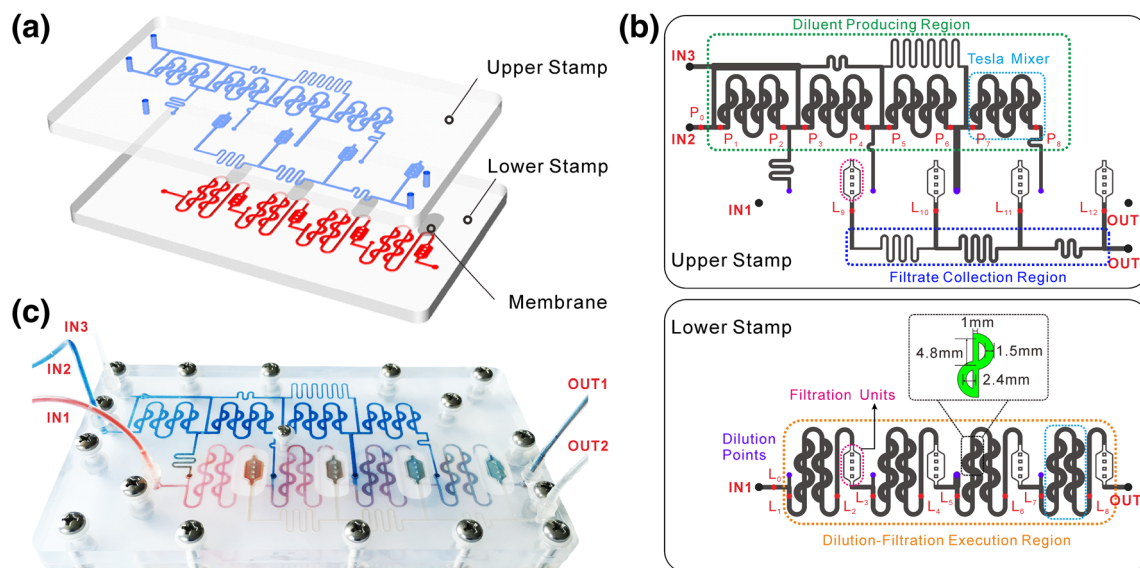


Fig. 1 Design of the multistep dilution-filtration microdevice (MDFD): **(a)** an exploded view of the MDFD; **(b)** the concept of the upper and lower stamps; **(c)** a photograph of the MDFD

points (Fig. 1b; dark purple points) was 2 mm. In the MDFD, a simplified version of the mixers in the literature (Kim et al. 2008) was used and the parameters of the mixers are shown in Fig. 1b. The polyvinylidene fluoride (PVDF) membranes (diameter of pores: ~ 0.45 , 0.8 and 1.2 μm ; thickness: ~ 100 μm ; Haiyan New Oriental Plastic Technology Co. Ltd., Jiaxing, China) were used for filtration. The silicone membrane (thickness: ~ 300 μm ; Shanghai Daoguan Rubber Hardware Co. Ltd., China) was used for sealing. The MDFD was assembled and then fixed with screws (Fig. 1c). Peristaltic pumps (YZ1515X; Baoding Longer Precision Pump Co. Ltd., China) were used to drive solutions to the MDFD.

2.3 Collection and glycerolization of cells

The collection and glycerolization of cells were performed as shown in our previous work (Zou et al. 2015). Briefly, the fresh porcine whole blood ($\sim 40\%$ Hematocrit; BanQiao Slaughter House, Hefei, China) was treated with the blood preserving solution (0.0275% w/v adenine, 0.222% w/v sodium dihydrogen phosphate, 0.327% w/v citric acid, 2.63% w/v sodium citrate, 3.19% w/v glucose; Sangon Biotech Co. Ltd., Shanghai, China) and stored at $4 \sim 8$ $^{\circ}\text{C}$. Then, the porcine red blood cells were separated and resuspended in an isotonic solution (0.9% w/v NaCl; ~ 290 mOsm/kg H_2O). Next, the compound glycerin solution (57% w/v glycerol, 0.2% w/v sodium hydrogen phosphate, 0.03% w/v potassium chloride, 3% w/v sodium lactate; Sinopharm Chemical Reagent Co. Ltd., Shanghai, China) was prepared as a mother solution. Finally, the red blood cell suspension with the desired cell density (in this study, the density of cells denotes Hematocrit and is the ratio of the total cell volume to the suspension volume) and

glycerin concentration was prepared by adding the diluted compound glycerin solution drop-by-drop to the responded cell suspension (the osmolalities of 20% and 40% w/v glycerin are approximately 2590 and 6380 mOsm/kg H_2O , respectively).

2.4 Pre-operation of the MDFD

Before experiments, deionized water was slowly introduced to **IN1**, **IN2**, and **IN3** to remove bubbles in the MDFD. Then, deionized water was replaced with a fluorescein solution (0.04 mM; Aladdin Industrial Corporation, Shanghai, China) to inspect the sealing under an inverted fluorescence microscope (Olympus IX53; American Inc., Center Valley, PA, USA).

In this work, after all experiments, the MDFD was washed by means of introducing the isotonic solution for 15 min and then deionized water for 15 min to **IN1**, **IN2**, and **IN3** at the designed flow rates. In addition, all experiments were conducted at least 3 times.

2.5 System fragility test

The MDFD itself may cause damage to cells. To assess the effect of MDFD, the system fragility test was performed. The glycerolized cell suspension (Hematocrit: 3% \sim 24%; Glycerin: 10% \sim 40%) was introduced to **IN1** and the corresponding glycerin solution (Glycerin: 10% \sim 40%) was introduced to **IN2** and **IN3**. Samples (0.40 mL) were collected after 15 min from **OUT1** and **OUT2** and then were analyzed (see Section 2.8).

2.6 Fluorescence experiments

In the first experiment, the glycerin solution (20% w/v), the fluorescein solution (0.04 mM), and deionized water were introduced to **IN1**, **IN2**, and **IN3**, respectively. After 15 min, fluorescence images at the positions **P₀** ~ **P₈** (Fig. 1b) were recorded using the inverted fluorescence microscope. In the second experiment, the solution with 0.04 mM fluorescein and 20% glycerin was introduced to **IN1** and deionized water was introduced to **IN2** and **IN3**. After 15 min, fluorescence images at the positions **L₀** ~ **L₁₂** (Fig. 1b) were recorded and the sample (0.40 mL) from **OUT1** was collected. The fluorescence intensity was analyzed using Matlab R2015a (The MathWorks, Inc., Natick, MA, USA). The concentration of glycerin was determined as shown in Section 2.8.

2.7 Deglycerolization of cells

In the experiments, the glycerin-loaded cell suspension (Hematocrit: 3% ~ 24%; Glycerin: 10% ~ 40%), the hypertonic solution (20% NaCl), the hypotonic solution (0% NaCl) were introduced to **IN1**, **IN2** and **IN3**, respectively (the pore size of the PVDF membrane was 0.45 ~ 1.2 μm). Samples (0.40 mL) were collected from **OUT1** and **OUT2** after 15 min. Then, they were analyzed to obtain the clearance of glycerin, the death rate of cells, and the recovery rate of cells (see Section 2.8).

2.8 Sample analysis

Glycerin concentration test The concentration of glycerin in samples was measured by a Beckman AU480 biochemical analyzer (Beckman Coulter; Tokyo, Japan) using a glycerin assay kit (Shanghai Shifeng Biological Technology Co. Ltd., Shanghai, China). First, 5 μL of the sample (diluted 1:4000) was mixed with 95 μL of the working solution prepared according to the assay kit specification (the sample with cells was centrifuged at 1000×g for 5 min and then the supernate was adopted in the test), and the mixture was incubated at 37 °C for 30 min. Then, the absorbance of the mixture and the standard glycerin sample was read at 550 nm by the analyzer. Finally, the concentration of glycerin in the sample was obtained by comparing the absorbance of the mixture with the absorbance curve of the standard glycerin samples.

Hemoglobin concentration test The concentration of hemoglobin in the collected samples was determined using a three-point Allen correction (Lusianti et al. 2013). The detailed procedure can be found in the previous work (Zou et al. 2015). In brief, by reading the absorbances A_{415} , A_{380} , and A_{450} of the supernate from the cell suspension (or from the lysed cell suspension) at 415 nm, 380 nm, and 450 nm, respectively, the concentration of hemoglobin (H_b ; mg/mL) can be obtained

(Han et al. 2010): $H_b = 0.1672A_{415} - 0.0836A_{380} - 0.0836A_{450}$. Thus, the death rate of cells and the recovery rate of cells can be estimated using the following equations.

Recovery rate of cells For the MDFD, the recovery rate of cells (R_C) was calculated by $R_C = (m_{OUT1}^{IH} / m_{IN1}^{IH}) \times 100\%$ (where m_{IN1}^{IH} and m_{OUT1}^{IH} are the intracellular quantities of hemoglobin in the samples collected at **IN1** and **OUT1**, respectively).

Survival rate of cells For the MDFD, the survival rate of cells (S_C) was calculated by $S_C = [1 - (m_{OUT1}^{EH} + m_{OUT2}^{EH} - m_{IN1}^{EH}) / m_{IN1}^{EH}] \times 100\%$ (where m_{IN1}^{EH} , m_{OUT1}^{EH} and m_{OUT2}^{EH} are the extracellular quantities of hemoglobin in the samples collected at **IN1**, **OUT1**, and **OUT2**, respectively). Then, the death rate of cells (D_C) was $[(m_{OUT1}^{EH} + m_{OUT2}^{EH} - m_{IN1}^{EH}) / m_{IN1}^{EH}] \times 100\%$.

Clearance of glycerin For the MDFD, the clearance of glycerin (C_G) was calculated by $C_G = (1 - C_{OUT1} / C_{IN1}) \times 100\%$ (where C_{OUT1} and C_{IN1} are the concentrations of glycerin in the samples collected at **OUT1** and **IN1**, respectively).

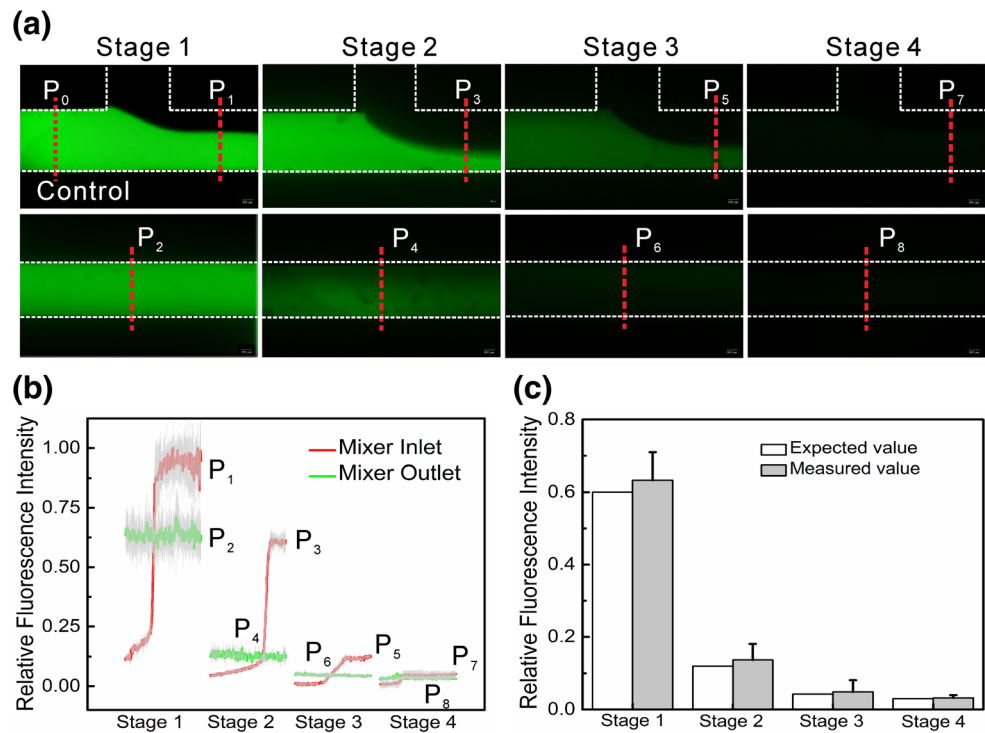
3 Results

3.1 Performance of the diluent producing region

In the MDFD, the diluent producing region on the upper stamp was composed of a ladder flow network with four mixers (Fig. 1b). The mixers were used to fully and quickly mix two merging solutions (concentrated NaCl solution and deionized water), and the ladder flow network was used to produce diluents with the desired NaCl concentrations and to introduce diluents at the desired flow rates. To verify the performance of the mixers, the glycerin solution (20%), fluorescein solution, and deionized water were introduced at the designed flow rates to **IN1**, **IN2** and **IN3** respectively (NaCl was substituted with fluorescein to facilitate the visualization of the mixing process). The fluorescence images were recorded before and after the mixers at the points **P₀** ~ **P₈** (Fig. 1b or Fig. S1; the relative fluorescence intensity = the fluorescence intensity / the fluorescence intensity at **IN2**). The images show that the distributions of fluorescein after the mixers were uniform (Fig. 2a). We further analyzed the relative fluorescence intensity before and after the mixers (Fig. 2b). The results indicate that the mixing was sufficient.

To confirm the performance of the ladder network, we compared the expected fluorescence intensities with the measured fluorescence intensities at four outlets of the ladder network. The measured values were close to the expected values (Fig. 2c). Thus, the ladder network we designed was capable to produce diluents with the desired NaCl concentrations.

Fig. 2 Performance of the diluent producing region: **(a)** the fluorescence images before (at points P_1, P_3, P_5, P_7) and after (at points P_2, P_4, P_6, P_8) the mixers; **(b)** distribution of the relative fluorescence intensities before and after the mixers; **(c)** comparison of the relative fluorescence intensities between the expected values and the measured values at four outlets of the ladder flow network



Because the NaCl concentrations prepared in diluents were related to the solution flow rates produced in the ladder network, the previous results imply that the ladder network can produce diluents at the desired flow rates for the dilution-filtration execution region.

3.2 Performance of the dilution-filtration execution region

In the MDFD, the dilution-filtration execution region on the lower stamp was composed of four mixers and four filtration units (Fig. 1b). The mixers were used to adequately mix the diluents from the diluent producing region and the glycerin-loaded cell suspension, and the filtration units were used to remove the extracellular glycerin solution. To verify the performance of the mixers, we introduced fluorescein-glycerin solution (glycerin: 20%; the fluorescein worked as an indicator) to IN1 and water to both IN2 and IN3, and then recorded the fluorescence images before and after the mixers at the points $L_0 \sim L_8$ (Fig. 1b or Fig. S1). The images in Fig. 3a and the relative fluorescence intensities in Fig. 3b show that the fluorescein solution and the dilution solution were fully mixed in the mixers. In addition, the measured fluorescence intensities were close to the expected values (Fig. 3c), indicating the mixers adopted were applicable.

To confirm the performance of the filtration units, we measured the fluorescence intensities and then calculated the clearance of fluorescein at the points $L_9 \sim L_{12}$ (Fig. 1b or Fig. S1). The results show that the measured clearances agreed with the expected clearances (Fig. 3d). To further confirm the

performance of removing glycerin, we compared the expected glycerin clearance with the measured glycerin clearance under the cell-free condition (Fig. 3e). The measured glycerin clearance was very close to the expected glycerin clearance. Thus, the performance of removing glycerin satisfied the design requirements.

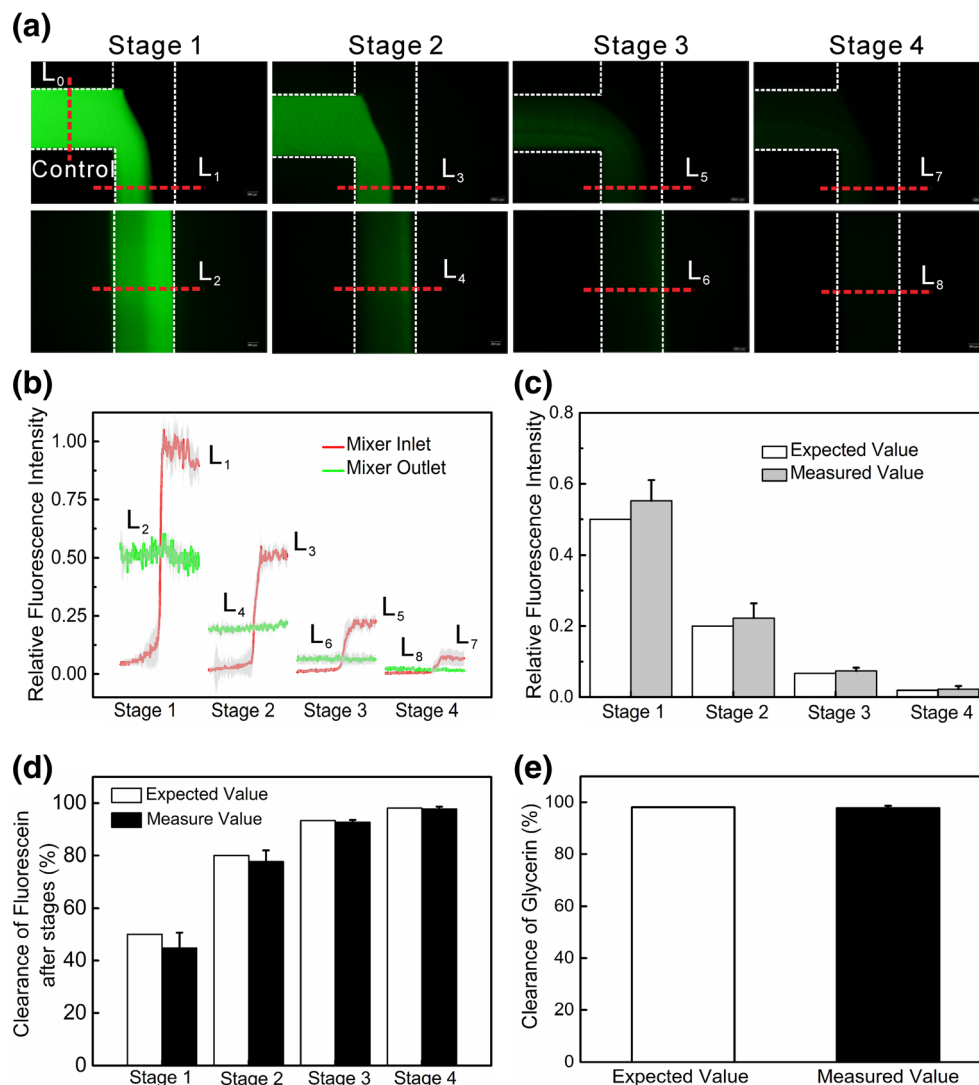
3.3 Effect of the MDFD structure on S_C and R_C

To assess S_C and R_C induced by the MDFD structure, the glycerolized cell suspension was introduced to IN1, and the glycerin solution was pumped to both IN2 and IN3. Then, S_C and R_C were analyzed (Fig. 4). S_C was very high (Fig. 4a, c), but R_C was low (Fig. 4b, d), indicating that the MDFD structure caused a very small death rate of cells but a large loss rate of cells. Moreover, even if the cell density and the glycerin concentration changed, S_C and R_C induced by the MDFD structure remained almost unchanged.

3.4 Performance of the MDFD

To study the performance of the MDFD when the glycerin-loaded cell suspension was introduced, we measured the performance indicators (C_G , S_C and R_C) under various cell densities, glycerin concentrations and membrane pore sizes (Fig. 5). The results show that the increase in either the cell density (Fig. 5a-c) or the pore size (Fig. 5g-i) caused the increase in C_G and the decrease in S_C and R_C while the

Fig. 3 Performance of the dilution-filtration execution region: **(a)** the fluorescence images before (at points L_1 , L_3 , L_5 , L_7) and after (at points L_2 , L_4 , L_6 , L_8) the mixers; **(b)** distribution of the relative fluorescence intensities before and after the mixers; **(c)** comparison of the relative fluorescence intensities between the expected values and the measured values at outlets of the mixers; **(d)** comparison of the fluorescein clearances between the expected values and the measured values at points L_9 , L_{10} , L_{11} , L_{12} ; **(e)** comparison of the glycerin clearance between the expected value and the measured value



increase in the glycerin concentration caused the decrease in all performance indicators (Fig. 5d-f).

4 Discussions

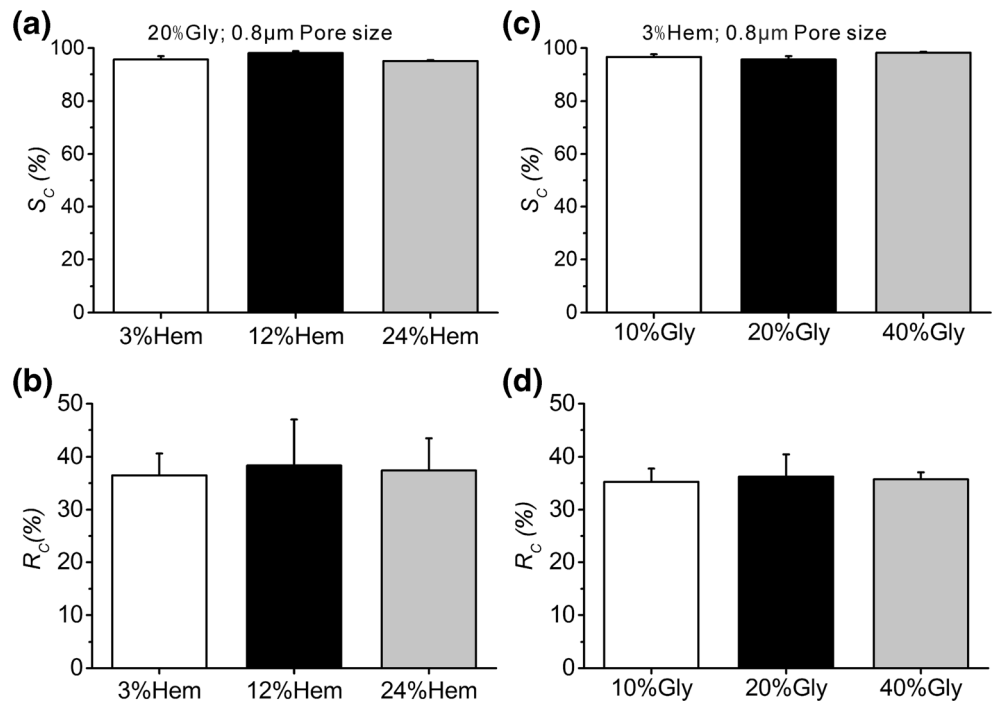
4.1 Effect of the mixers

The mixers we used showed good mixing performance as they fully and quickly mixed two emerging solutions (Fig. 2a, b and Fig. 3a, b). In the dilution-solution producing region, if the performance of mixers is bad, deionized water and concentrated solution will not be fully mixed, and then the concentration of NaCl in the prepared dilution solution will depart from the expected value. Thus, the osmotic damage to cells may happen because of the concentration deviation. Consequently, the death rate of cells and then the recovery rate of cells will be affected. Because the glycerin inside of cells damaged will be quickly transferred to the surrounding

solution, the expected concentration of glycerin in the network and then the expected clearance of glycerin will be changed. The change in the concentrations of glycerin in the network will cause the change in the flow resistances and then the change in the flow rates in the entire microsystem. Thus, the NaCl and CPA concentrations will further deviate from the designed values, causing the large changes in the clearance of glycerin, the death rate of cells, and the recovery rate of cells.

In the dilution-filtration execution region, the mixers are to quickly mix the glycerin-loaded cell suspension and the prepared dilution solution and to provide a friendly environment for cells so that the glycerin inside cells can be transported to the solution around cells. Thus, in addition to a high mixing efficiency, the mixer length should be long enough to guarantee the residence time of cells for the glycerin transport. We simulated the change in the concentration of glycerin inside cells in the entire microsystem (Fig. S2a). The results indicate that the length of the mixers we used was proper because the

Fig. 4 Effect of the MDFD structure on S_C and R_C : **(a)** S_C under various Hematocrits; **(b)** R_C under various Hematocrits; **(c)** S_C under various glycerin concentrations; **(d)** R_C under various glycerin concentrations (Gly: glycerin; Hem: Hematocrit)



concentration of glycerin inside cells always decreased to a value close to the expected one after dilution. Here, the mixers were designed to be the same. In practice, one may customize the length of the mixers according to the time required for the

concentration of glycerin inside cells decreasing to the expected value so that the MDFD can be further miniaturized.

In this study, to simplify the design process, the effect of fluxes on the flow resistances in the mixers and the effect of

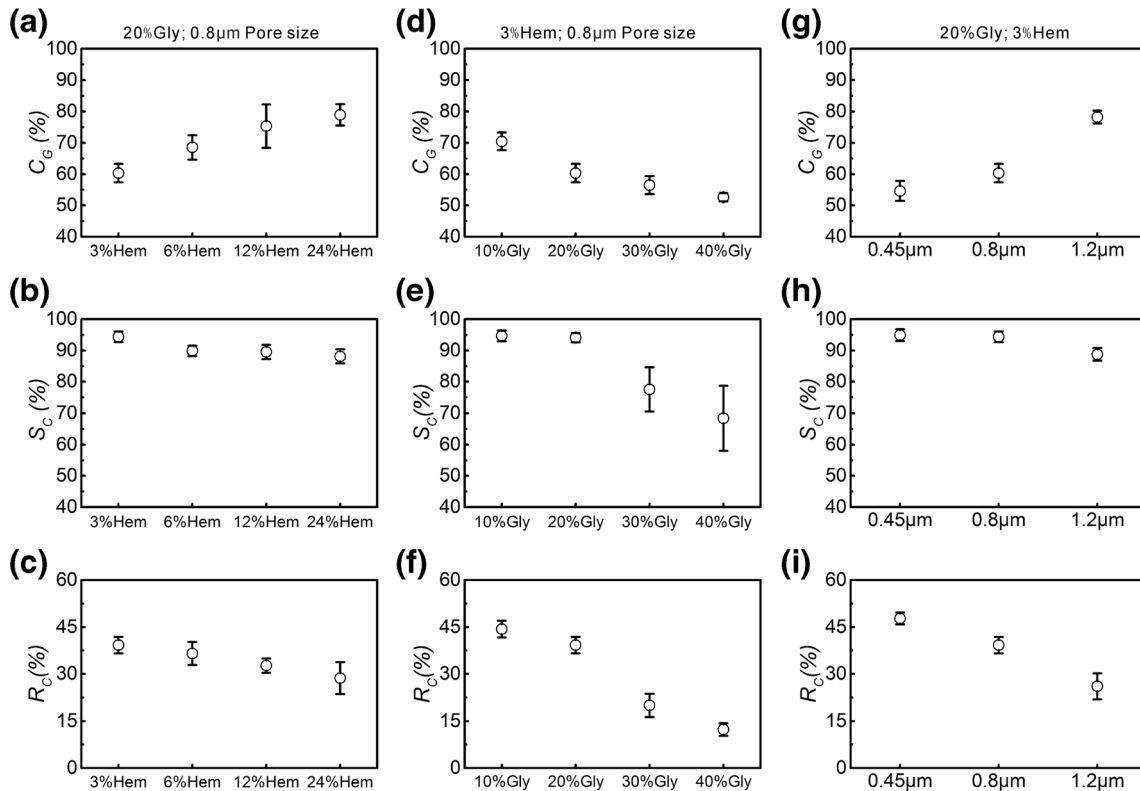


Fig. 5 Performance of the MDFD: **(a-c)** C_G , S_C , and R_C under various Hematocrits; **(d-f)** C_G , S_C , and R_C under various glycerin concentrations; **(g-i)** C_G , S_C , and R_C under various membrane pore sizes

viscosities on the flow resistances in the network were not considered. Thus, the flow rate and solute concentration in the entire microsystem deviated from the expected values. To reduce the deviation induced by the simplification, we added a pump at **OUT2** to adjust the flow rate through **OUT2** in experiments so that the flow rate through **OUT1** was the same as the flow rate through **IN1**. The results show that in the cell-free experiments, the measured values agreed with the expected ones (Fig. 2c and Fig. 3c-e). Therefore, it is feasible to partially correct the intra-systemic fluxes and concentrations by means of adding a pump at **OUT2**.

4.2 Effect of the filtration operation

In the MDFD design, we adopted a way akin to the membrane-based blood plasma separation (Aran et al. 2011; Thorslund et al. 2006) to filter out the solution around cells. Thus, the microsystem we developed had an intrinsic shortcoming derived from the membrane-based separation. That is, because of the suction of the filtrate collection region, a fraction of cells was detained on the membrane surface and some of them were squeezed through the membrane pores into the filtered solution. Therefore, R_C was a little low (Fig. 4b, d). Because a fraction of cells blocked the membrane pores, the glycerin clearances in cell experiments (Fig. 5a, d, g) were all smaller than the clearances in cell-free experiments (Fig. 3e). To reduce the blockage of cells on the membrane surface, one may embed a passive cell separation design, e.g. constriction-expansion design (Marchalot et al. 2014; Sollier et al. 2010) and Zweifach-Fung design (Kersaudy-Kerhoas et al. 2010; Tripathi et al. 2013), before the filtration procedure. Thus, a part of the solution around cells is separated beforehand and then filtrated by the membrane. Consequently, the recovery rate of cells can be increased and then the desired clearance of glycerin can be reached. In fact, the introduction of a passive design into the MDFD can bring another advantage. That is, the MDFD can be repeatedly used.

4.3 Effect of the stage number

The stage number (the number of the dilution-filtration operation) affects not only the size of the MDFD (the more the stage number is, the bigger the MDFD size is), but also the death rate of cells and the recovery rate of cells. If the stage number is small, the ratio of the dilution solution flow rate (the filtrate flow rate) to the mixed cell suspension flow rate ($Q_{d,i}/Q_{n,i} = Q_{f,i}/Q_{n,i}$) must be large to make the concentration of glycerin down to a given expectation. In this case, the osmotic damage to cells will be high and then the death rate of cells will be large. In addition, the number of cells detained on the membrane surface also will be large, especially when the flow rate of the mixed cell suspension is small. Thus, the recovery rate of cells will be low. If the stage number is large, the ratio

can be small. Then, the number of the cells detained and damaged osmotically will be little; however, the size of MDFD will be large. Therefore, in the design of the stage number, the size of MDFD, the death rate of cells and the retention rate of cells should be considered as a whole. Here, we adopted the stage number four. The results show S_C was high (Fig. 5b, e, h) but R_C was relatively low (Fig. 5c, f, i). Thus, there is a large space for the performance optimization of the MDFD by adding the stage number.

4.4 Effect of the operating conditions

For the MDFD, the operating conditions, i.e. the glycerin concentration in the cell suspension, the cell density, and the membrane pore size can significantly affect the clearance of glycerin, the death rate of cells and the recovery rate of cells (Fig. 5).

If the density of cells is high, the extracellular concentration of glycerin will be low after dilution. Thus, the difference of the concentration of glycerin across the cell membrane will be high and then a large quantity of glycerin inside cells will be removed. Therefore, the higher the density of cells is, the higher C_G is (Fig. 5a). If the density of cells is high, the viscosity of the cell suspension and then the pressure difference across the filtration membrane will be large. Thus, a large number of cells will be detained on the membrane surface, and some of them may be squeezed through the membrane pores into the filtrate, especially when the membrane pore size is large. Consequently, R_C is lower at a higher density of cells (Fig. 5c). Because the cells squeezed through the membrane pores may be broken, S_C is also lower at a higher density of cells (Fig. 5b).

If the concentration of glycerin to be removed in the cell suspension is higher, the viscosity of the cell suspension will also be higher. Thus, the number of the cells detained on the membrane surface and squeezed through the membrane pores into the filtrate will be larger and then R_C is lower (Fig. 5f). Because a larger number of the cells detained will block the filtration membrane pore, C_G is lower at a higher glycerin concentration (Fig. 5d). In addition, a larger number of the cells squeezed through the membrane pores may be broken; thus, S_C is also lower at a higher glycerin concentration (Fig. 5e). It should be noted that the dead cells here contained not only the cells damaged osmotically but also the cells broken during the membrane filtration process.

If the pore size of the filtration membrane is larger, the transport of glycerin across the filtration membrane is easier and thus C_G will be larger (Fig. 5g). However, a larger pore size will cause a larger number of the cells to be detained on the membrane surface and squeezed through the membrane pores into the filtrate. Consequently, both S_C (Fig. 5h) and R_C (Fig. 5i) will be lower (the high cleaning efficiency of glycerin at a high density of cells or a large pore size may be partly responsible for the decrease in S_C as it cause the large glycerin

concentration difference across the cell membrane and then the large osmotic damage to cells).

Here, the MDFD was designed under fixed flow rates; thus, it is better to operate the microdevice under invariable flow rates rather than under variable flow rates as shown in the microsystems of the literature (Scherr et al. 2013; Scherr et al. 2014). If the cell suspension flow rate in the MDFD is varied, the flow rates of hypertonic and hypotonic solutions also need to be varied. Thus, the flow rates, the NaCl concentrations, and the CPA concentrations in the entire microsystem will be varied. Consequently, the performance of the MDFD will deviate from the expectation.

In the MDFD design, the selection of the cell suspension flow rate should be proper. If the cell suspension flow rate is large, the MDFD size will be large. In addition, the large cell suspension flow rate means the large flow rates of dilution solutions and then the large flow rates of filtrates through membrane. However, the large flow rates of dilution solutions will cause the large quantity of cells detained and they are also practically restricted by membrane permeability. Thus, the design of the cell suspension flow rate should consider the system size, the cell retention, and the membrane performance.

4.5 Factors affecting the performance of the MDFD

For the MDFD, C_G is dominated by the product $\prod_{i=1}^4 \frac{Q_{e,i}}{Q_{e,i} + Q_{d,i}}$. Here, the designed ratios $\frac{Q_{d,1}}{Q_{e,1}}$, $\frac{Q_{d,2}}{Q_{e,2}}$, $\frac{Q_{d,3}}{Q_{e,3}}$ and $\frac{Q_{d,4}}{Q_{e,4}}$ were 1.0, 1.5, 2, and 2.5, respectively. Thus, C_G theoretically is 98% (the expected value can be reached only when the density of cells is 0, as shown in Fig. 3e). However, due to the blockage of the cells detained on the membrane, it was only 80% under the setting conditions. S_C is affected by two factors: one is the osmotic damage to cells during the dilution process, and the other is the crush damage to cells during the filtration process. The osmotic damage to cells can be controlled by the ratio $\frac{Q_{d,i}}{Q_{e,i}}$ and the NaCl concentration in the dilution solution $C_{d,i}$. The simulation show that the designed ratio and concentration made the volume of cells always in the range of the upper and lower volume tolerance limits (Fig. S2b). Then, the osmotic damage to cells in the MDFD is little under the setting conditions. However, due to the usage of the large pore membrane, the crush damage to cells happened (Fig. 5b, e, h), causing ~5% of cells dead under the setting conditions. R_C is affected by the filtration process, as discussed previously.

5 Conclusions

We presented a multistep dilution-filtration microdevice (MDFD) to unload CPAs from a small amount of the CPA-

loaded cell samples. For the MDFD designed here, under the setting conditions (the cell suspension flow rate is 0.2 mL/min, the glycerin concentration is 20% w/v and the cell density is 24% v/v), C_G can reach ~80% and S_C can achieve ~90%. However, R_C is only ~40%, mainly resulting from some cells detained on the membrane surface and squeezed into the filtrate in the filtration process. By adopting the large pore membrane, C_G can be increased but both S_C and R_C will decrease. The MDFD shows a better performance under a lower concentration of glycerin. In addition, if a high density of cells is applied, although C_G is high, both S_C and R_C are low.

The core design adopted in the MDFD is the same as the one developed in the previous macro-system (Zhou et al. 2011). Thus, the MDFD also shows good performances with respect to S_C and C_G . However, because of the usage of the large pore membrane, R_C here is lower. Compared to existing microsystems, the MDFD significantly reduces the death rate of cells and increases the clearance efficiency of glycerin. In this study, although the MDFD designed is promising, the approaches to reducing the number of the cells detained on the membrane surface and squeezed through the membrane pores into the filtrate are urgently needed in the future. First, one may add a passive cell separation design before the filtration. Thus, a large portion of cells is separated beforehand and bypasses the filtration membrane. Second, the small pore membrane is highly recommended. Third, the number of stages can be properly increased. Forth, the high flow rate of the cell suspension through the membrane surface should be better. Here, the size of the MDFD we designed is a little big. In the future, one may design multilayer stamps to further miniaturize the MDFD.

Acknowledgments This work was partially supported by the National Natural Science Foundation of China (Grant Nos.: 81571768, 81627806), the Fundamental Research Funds for the Central Universities (Grant Nos.: WK6030000054, WK3490000001), and the Specialized Research Fund for the Doctoral Program of Higher Education of China (Grant No.: 20133402120033). The funders had no role in the study design, data collection and analysis, decision to publish, or preparation of the manuscript.

Compliance with ethical standards

Conflict of interest The authors declare no conflict of interest.

References

- K.A. Almansoori, V. Prasad, J.F. Forbes, G.K. Law, L.E. McGann, J.A.W. Elliott, N.M. Jomha, *Cryobiology* **64**, 185 (2012)
- K. Aran, A. Fok, L.A. Sasso, N. Kamdar, Y.L. Guan, Q. Sun, A. Undar, J.D. Zahn, *Lab Chip* **11**, 2858 (2011)
- T.P. Burg, M. Godin, S.M. Knudsen, W. Shen, G. Carlson, J.S. Foster, K. Babcock, S.R. Manalis, *Nature* **446**, 1066 (2007)

- W. Ding, J. Yu, E. Woods, S. Heimfeld, D. Gao, J. Membr. Sci. **288**, 85 (2007)
- R. Dou, R.E. Saunders, L. Mohamet, C.M. Ward, B. Derby, Lab Chip **15**, 3503 (2015)
- S. Ferrari, A. Paffoni, F. Filippi, A. Busnelli, W. Vegetti, E. Somigliana, Reprod. BioMed. Online **33**, 29 (2016)
- E. Fitzpatrick, S. Xu, J. Datta, J. Cintolo, B. Czerniecki, Cytotherapy **17**, S22 (2015)
- K.K. Fleming Glass, E.K. Longmire, A. Hubel, Int. J. Heat Mass Tran **51**, 5749 (2008)
- L. Gong, W. Ding, Y. Ma, S. Sun, G. Zhao, D. Gao, Biopreserv. Biobank. **11**, 299 (2013)
- V. Han, K. Serrano, D. Devine, Vox sanguinis **98**, 116 (2010)
- J. Hanna, A. Hubel, E. Lemke, Biotechnol. Bioeng. **109**, 2316 (2012)
- Y.S. Heo, H.J. Lee, B.A. Hassell, D. Irimia, T.L. Toth, H. Elmoazzen, M. Toner, Lab Chip **11**, 3530 (2011)
- R. Hoyt, J. Szer, A. Grigg, Bone Marrow Transpl **25**, 1285 (2000)
- A. Hubel, Transfusion **51**(Suppl 4), 82S (2011)
- S. Jadoon, M. Adeel, J Ayub Med Coll Abbottabad **27**, 22 (2015)
- M. Kersaudy-Kerhoas, D.M. Kavanagh, R.S. Dhariwal, C.J. Campbell, M.P. Desmulliez, Lab Chip **10**, 1587 (2010)
- C. Kim, K. Lee, J.H. Kim, K.S. Shin, K.J. Lee, T.S. Kim, J.Y. Kang, Lab Chip **8**, 473 (2008)
- E.K. Longmire, J. Biomech. Eng-T. Asme **129**, 703 (2006)
- R.E. Lusianti, A.Z. Higgins, Biomicrofluidics **8**, 054124 (2014)
- R.E. Lusianti, J.D. Benson, J.P. Acker, A.Z. Higgins, Biotechnol. Prog. **29**, 609 (2013)
- J. Marchalot, Y. Fouillet, J.L. Achard, Microfluid. Nanofluid. **17**, 167 (2014)
- C. Mata, E.K. Longmire, D.H. McKenna, K.K. Glass, A. Hubel, Microfluid. Nanofluid. **5**, 529 (2008)
- C. Mata, E. Longmire, D. McKenna, K. Glass, A. Hubel, Microfluid. Nanofluid. **8**, 457 (2009)
- H.T. Meryman, Transfusion **47**, 935 (2007)
- S. Park, P.A. Wijethunga, H. Moon, B. Han, Lab Chip **11**, 2212 (2011)
- D.G. Pyne, J. Liu, M. Abdelgawad, Y. Sun, PLoS One **9**, e108128 (2014)
- H. Qiao, W. Ding, S. Sun, L. Gong, D. Gao, Biomed. Eng. Online **13**, 120 (2014)
- V. Ragsdale, H. Li, H. Sant, T. Ameel, B.K. Gale, Biomed. Microdevices **18**, 1 (2016)
- T. Scherr, S. Pursley, W.T. Monroe, K. Nandakumar, Biomicrofluidics **7**, 024104 (2013)
- T. Scherr, S. Pursley, W. Todd Monroe, K. Nandakumar, Int. J. Heat Mass Tran **78**, 1284 (2014)
- E. Sollier, M. Cubizolles, Y. Fouillet, J.L. Achard, Biomed. Microdevices **12**, 485 (2010)
- Y.S. Song, S. Moon, L. Hulli, S.K. Hasan, E. Kayaalp, U. Demirci, Lab Chip **9**, 1874 (2009)
- R. Syme, M. Bewick, D. Stewart, K. Porter, T. Chadderton, S. Glück, Biol. Blood. Marrow. Tr **10**, 135 (2004)
- S. Thorslund, O. Klett, F. Nikolajeff, K. Markides, J. Bergquist, Biomed. Microdevices **8**, 73 (2006)
- S. Tripathi, A. Prabhakar, N. Kumar, S.G. Singh, A. Agrawal, Biomed. Microdevices **15**, 415 (2013)
- T.-R. Wang, J. Yan, C.-L. Lu, X. Xia, T.-L. Yin, X. Zhi, X.-H. Zhu, T. Ding, W.-H. Hu, H.-Y. Guo, Hum. Reprod. **31**, 763 (2016)
- K.W. Yong, W.K.Z. Wan Safwani, F. Xu, W.A.B. Wan Abas, J.R. Choi, B. Pinguan-Murphy, Biopreserv. Biobank **13**, 231 (2015)
- W. Zhang, G. Yang, A. Zhang, L.X. Xu, X. He, Biomed. Microdevices **12**, 89 (2010)
- X. Zhou, Z. Liu, Z. Shu, W. Ding, P. Du, J. Chung, C. Liu, S. Heimfeld, D. Gao, J Biomech Eng **133**, 021007 (2011)
- L. Zou, W. Ding, S. Sun, F. Tang, D. Gao, Cryobiology **71**, 210 (2015)